100 YEARS Journal of Ecology

British Ecological Society

Journal of Ecology doi: 10.1111/1365-2745.12297

Long-term expansion of juniper populations in managed landscapes: patterns in space and time

Cristina García[1]*, Eva Moracho[2], Ricardo Díaz-Delgado[3] and Pedro Jordano[2]

[1]*Plant Biology, Centro de Investigação em Biodiversidade e Recursos Genêticos (CIBIO/InBio), Campus Agrário de Vairão, Rua Padre Armando Quintas, Vairão 4485-661, Portugal;* [2]*Integrative Ecology Group, Estación Biológica de Doñana Consejo Superior de Investigaciones Científicas (EBD-CSIC), Avenida Americo Vespucio s/n, Sevilla E-41092, Spain; and* [3]*Remote Sensing and GIS Lab, Estación Biológica de Doñana, Consejo Superior de Investigaciones Científicas (EBD-CSIC), Avenida Americo Vespucio s/n, Sevilla E-41092, Spain*

Summary

1. Forest cover has increased world-wide over the last decade despite continuous forest fragmentation. However, a lack of long-term demographic data hinders our understanding of the spatial dynamics of colonization in remnant populations inhabiting recently protected areas or set-aside rural lands.

2. We investigated the population expansion of the Phoenician juniper (*Juniperus phoenicea* subsp. *turbinata*), which is an endozoochorous Mediterranean tree species inhabiting landscapes that have been managed for many centuries. By combining the photointerpretation of aerial photos that have been taken over the last 50 years with *in situ* sampling and spatial analyses of replicated plots, we estimated the population growth over the chronosequence; identified hotspots, coldspots and outliers of regeneration; and assessed the roles of key environmental factors in driving demographic expansion patterns, including elevation, initial density and distance to remnant forests.

3. Ecological factors leading to seed limitation, such as initial plant density, are expected to drive colonization patterns at the early stages. Factors mediating the competition for limiting resources, such as water availability, would prevail at later stages of expansion. We further expect that nucleated colonization patterns emerge driven by vertebrate seed dispersal.

4. The photointerpretation of aerial images in combination with *in situ* measurements has yielded reliable density data. Overall, our results show a marked demographic expansion during the first decade followed by a period of steady and heterogeneous population growth with signs of local population decline. We found evidence of nucleated establishment patterns as expected for an endozoochorous species. Hotspots and outliers of regeneration emerged throughout the study chronosequence, whereas coldspots of regeneration only appeared at advanced colonization stages. Factors influencing dispersal limitation had contrasting effects at different colonization stages, and the initial density influenced population growth at various spatial scales.

5. *Synthesis*. The photointerpretation of aerial images shows that the influence of dispersal limitation versus factors mediating competitive responses changes throughout colonization stages. Whereas dispersal limitation is the main factor influencing colonization at early stages, competition for local resources controls population growth at later stages. Therefore, long-term studies are required to capture the overall combined influence of key ecological factors in shaping long-term spatial demographic trends.

Key-words: ecological correlates, generalized additive mixed models, historical forest fragmentation, *Juniperus phoenicea* subsp. *turbinata*, long-term demographic trends, photointerpretation, plant population and community dynamics, spatial statistics

Introduction

Factors underlying environmental change, such as the loss of seed dispersal vectors, landscape fragmentation and habitat disruptions, have limited the pace and extent of natural regeneration (Kareiva, Kingsolver & Huey 1993; Markl *et al.* 2012). However, forest cover has increased worldwide over the last decade (Leadley *et al.* 2010). Mediterranean forest species have exhibited variable recovery rates, and remnant populations being located in abandoned rural lands or protected

*Correspondence author: E-mail: cristinagarcia@cibio.up.pt

© 2014 The Authors. Journal of Ecology © 2014 British Ecological Society

areas have experienced the largest demographic expansions. Nevertheless, little attention has been given to the natural regeneration and colonization patterns of remnant forests, such as those that are located in the Mediterranean basin, which are factors that are extremely important for the prediction of their chances of persisting and expanding (Clark *et al.* 2001). Long-term data describing the population dynamics of tropical and temperate forests are currently available (Condit *et al.* 1999; Foster 2002; Ladwig & Meiners 2010), but studies on the regeneration dynamics of remnant Mediterranean forests are limited to reduced spatiotemporal scales. Protected areas containing remnant forests offer a unique opportunity for long-term ecological studies investigating the demographic responses of woody forest species to land-use changes in semi-arid Mediterranean environments.

Both biotic and abiotic factors influence long-term regeneration dynamics (Watt 1947). First, biotic interactions, such as dispersal mutualisms and facilitation among nearby individuals, strongly shape the initial recruitment stages (Seidler & Plotkin 2006; Hampe *et al.* 2008). For example, endozoochorous species tend to show nucleated colonization patterns because frugivorous vertebrates deposit large numbers of dispersed seeds under sites that have been selected for feeding or perching, such as conspicuous fruiting trees, whereas propagules rarely reach sites that are avoided by dispersal vectors (Verdú & García-Fayos 1996). These hotspots and coldspots of dispersed seeds tend to become hotspots and coldspots of regeneration (Hampe *et al.* 2008) if subsequent demographic processes do not drown out the early signals that are derived from highly clumped seed rains. Second, the spatial distribution of safe sites for germination and survival drives late recruitment stages (Yarranton & Morrison 1974). For example, Getzin *et al.* (2008) reported that new recruits and adults were aggregated around a few safe sites in secondary forests that possessed high environmental heterogeneity, whereas uniform recruitment patterns emerged in environmentally homogeneous communities. Thus, the roles of biotic and abiotic environmental factors may change along the recruitment cycle, which are often associated with opposing effects on survival at different stages (Schupp 1995). However, most previous studies are confined to a single or several demographic stages, failing to capture the overall combined influences of key ecological drivers in shaping long-term spatial demographic trends.

Pattern-driven studies track population trends at the landscape level, and ideally, although rarely, along an extensive chronosequence. The photointerpretation of satellite images or aerial photos is a suitable tool for the acquisition of demographic data spanning several decades for populations that inhabit changing landscapes (Díaz-Delgado 2010; Fretwell *et al.* 2012). This is the case for stands of long-lived tree species, such as the juniper woodlands (*Juniperus phoenicea* subsp. *turbinata*) at the Reserva Biológica de Doñana (RBD, SW Spain), which is an area with a history of traditional management that was declared to be a protected national park in 1969.

Previous work has shown that soil moisture and species composition changed through successional time following abandonment from deforestation (Allier, González & Ramirez 1974; García-Novo & Merino 1997; Muñoz-Reinoso 2001; Suarez-Esteban, Delibes & Fedriani 2013). Moreover, remnant patches of juniper trees successfully colonized the surrounding areas that are dominated by woody shrubs as a result of the active mobilization of propagules by medium- to large-sized frugivorous vertebrates, such as birds and mammals. Junipers are considered to be the foundation species according to Whitham *et al.* (2006) of Mediterranean semi-arid ecosystems, and previous studies have shown that adult and juvenile trees can be identified on an individual basis by the photointerpretation of aerial photos (Díaz-Delgado 2010). Therefore, this juniper species provides an ideal system with which to investigate the spatial dynamics of an expanding population by bridging the photointerpretation of aerial images that have been taken over the course of several decades with spatial statistics and ecological modelling.

Here, we investigate the spatio-temporal expansion patterns of a juniper woodland population inhabiting a recently protected, but formerly managed for centuries, landscape. We wish to elucidate the roles of different ecological factors in driving colonization patterns over a chronosequence spanning 1956–2005. Previous studies in the same area have shown that the demographic expansion of several woody species outside of the remnant juniper woodlands is driven by the dispersal activities of medium-sized frugivorous birds (Jordano 1993) and mammals (Suarez-Esteban, Delibes & Fedriani 2013). Competition for resources (typically soil moisture in Mediterranean semi-arid environments (Williams *et al.* 2010)) increases as local density grows, and therefore, it may underlie expansion patterns at late colonization stages. The photointerpretation of aerial images also gauges the spatial variation of key ecological factors that potentially control population growth at the landscape scale, such as the distance to remnant forests and the initial density (both as proxies of dispersal limitation) and elevation (a proxy of soil moisture). We predict that the importance of these ecological factors changes between colonization stages, potentially confounding the interpretation of factors driving long-term trends. Specifically, we expect that nucleated patterns should emerge at the colonization front as a consequence of active but highly aggregated dissemination by frugivores. Additionally, factors implying seed limitation, such as the initial density (source limitation) or the distance to the core of the remnant forest (dispersal distance limitation) (Schupp, Milleron & Russo 2002), would drive the initial stages of the colonization. Finally, factors implying competition for resources, such as soil moisture, would prevail at later stages of expansion. To track the colonization patterns and decipher the roles of the ecological factors underlying the observed spatio-temporal population dynamics, we accomplished the following:

1 The estimation of the density variation across the landscape according to the interpretation of aerial photos that were taken from 1956 to 2005;

2 The identification of distinct sites of increased population growth (hotspots and outliers of regeneration) and other sites

exhibiting decreasing trends of density variation (coldspots and gaps of regeneration) across the landscape based on spatial statistics;

3 The assessment of key ecological correlates potentially influencing population dynamics across the landscape using aerial photos. We measured the initial density at the beginning of the study chronosequence (a proxy of seed limitation), the distance to the remnant forest (a proxy of dispersal limitation), and the elevation (a proxy of water availability);

4 The modelling and testing of the effects of these ecological correlates in determining population density variation over the study chronosequence and across the landscape.

Materials and methods

STUDY SPECIES

The Phoenician juniper *Juniperus phoenicea* subsp. *turbinata* (Guss.) Nyman (Cupressaceae) is a woody gymnosperm species inhabiting coastal dunes, paleodunes and rocky seashores in the western Mediterranean and several islands in the Macaronesian archipelagos (Adams 2011). This species is well adapted to harsh coastal environments with marked summer droughts, salty and windy environments and poor soils. It is a monoecious species, but several populations show functionally subdioecious mating systems in which most individuals mainly produce either female or male cones (Jordano 1991). It is an anemophilous species and sheds pollen from the end of September to November. Its reproductive cycle spans 2 years, and adult trees produce ripe, brown-coloured, berrylike arcestides with seeds that are dispersed by medium- to large-sized vertebrates from October to February. The most relevant seed dispersers include several thrush species, such as *Turdus philomelos*, *T. merula* and *T. iliacus* (Jordano 1993), and mammals, such as badgers (*Meles meles*), foxes (*Vulpes vulpes*) (Rau 1987; Fedriani & Delibes 2009), rabbits (*Oryctolagus cuniculus*) (Dellafiore, Valles & Fernandez 2006) and lizards (*Lacerta lepida*) (P. Jordano, pers. obs.).

STUDY AREA AND SAMPLING DESIGN

The Reserva Biológica de Doñana (RBD) is located within the limits of the Doñana National Park (SW Spain, 36°56′51″ N 6° 21′31″ W Fig. 1a). This area was traditionally managed until it was declared a national park in 1969. Extensive cattle ranches and stone pine (*Pinus pinea*) plantations were economically important to this region, and hunting, fishing and the gathering of natural goods were also vital to its inhabitants. This area has a Mediterranean climate with oceanic influences, a mean winter temperature of approximately 11.8 °C and mean summer temperatures reaching 23.0 °C. Annual rainfall averages 550 mm with two main wet periods during the spring (March–April) and autumn (October–November) seasons. The RBD is composed of three main landscape units (Valverde 1958), including marshes, beaches and mobile dunes, and stabilized dunes. The study area is located on the southwest border of the RBD and is dominated by stabilized dunes that are oriented NE–SW following the coastal dune line (Fig. 1b). This area consists of a set of dry elevated crests (20–40 m) with mesic intercrest depressions. The crests and intercrest depressions differ in their depths to the water-table and, consequently, host different plant communities (González-Bernáldez, García-Novo & Ramírez 1975a,b; Rivas-Martínez *et al.* 1980). Stabilized crests with summer phreatic level at depths of 3 m are dominated by J. *p. turbinata* Guss., *Halimium commutatum* Pau, *H. halimifolium* L., *Rosmarinus officinalis* L. and *Cistus libanotis* L. The intercrest depressions with the summer phreatic levels of 0–1.5 m in depth are dominated by *Erica scoparia* L., *Erica ciliaris* L., *Ulex minor* Roth, *Calluna vulgaris* L., *Phillyrea angustifolia* L. and *Cistus salvifolius* L. Intermediate steep zones with summer phreatic levels of between 1.5 and 3 m are dominated by *H. halimifolium* L. and *Ulex australis* Clemente.

This study was conducted at two different sites that are located 1.5 km apart on the stabilized *Sabinar del Marqués* and *Sabinar del Ojillo* dune crests (Fig. 1c). The first site consists of a large and dense monospecific mature stand with a mean density of 1100 individuals per hectare occupying an area of 50 ha with a mean elevation of 29.7 m (±2.9 SD) that is surrounded by a stone pine reforestation (*Pinus pinea*) and Mediterranean scrubland with *H. commutatum*, *H. halimifolium*, *R. officinalis* and *C. libanotis*. *Sabinar del Ojillo* consists of a mixed forest patch (15 ha) that is composed of juniper trees (mean density of 813 ind ha^{-1}) and sparsely distributed stone pine trees (Granados, Martín & García-Novo 1988) with a mean elevation of 19.8 m (±4.2 SD) surrounded by pine reforestation lands and Mediterranean scrublands of *E. scoparia*, *E. ciliaris*, *U. minor*, *C. vulgaris*, *P. angustifolia* and *C. salvifolius.*

We set one plot at each of the study sites, which are hereafter referred to as MAR (1140 × 900 m) and OJI (1140 × 700 m). We sampled subplots of increasing areas (100 m^2, 400 m^2 and 1600 m^2) within each plot to identify the subplot size yielding the most reliable

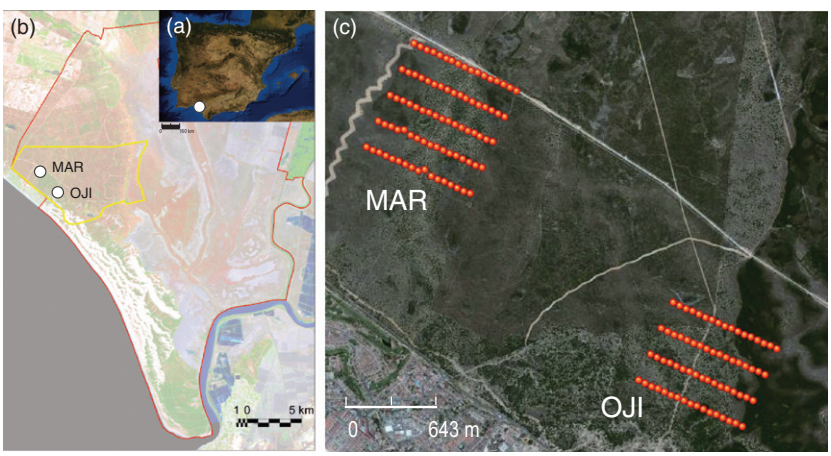

Fig. 1. (a) Location of the Doñana National Park in the Iberian Peninsula (white spot). (b) Limits of Doñana National Park (red line), limits of the Reserva Biológica de Doñana (yellow line) and the locations of the study plots, which are referred to as MAR (located at Sabinar del Marqués) and OJI (located at Sabinar del Ojillo). (c) Locations of the study plots and the spatial distributions of the subplots (red dots) along 5 transects in MAR and 4 transects in OJI.

© 2014 The Authors. Journal of Ecology © 2014 British Ecological Society,

density estimates. We determined that a subplot size of 400 m^2 minimises sampling efforts while providing robust estimates of mean density with reduced variances across different measurements. Then, we set 85 subplots at MAR and 68 subplots at OJI (Fig. 1c), which were located along 5 transects at MAR and 4 transects at OJI of 1140 m in length at NW-SE orientations and with an intertransect distances of 200 m. These subplots represented the units of this study.

ESTIMATIONS OF DENSITY VALUES BASED ON INTERPRETATIONS OF AERIAL IMAGES

Our analysis of the spatio-temporal demographic trends was based on the interpretation of three aerial images of the study area that were obtained from 1956 to 2005 and included three main goals as follows: (i) the georeferencing of orthophotos from 1956, 1977 and 2005; (ii) the identification of juniper trees on an individual basis and estimations of juniper densities in each subplot that were based on each previously georeferenced orthophoto; and (iii) the *in situ* validation of density estimates. We estimated the juniper density in each subplot within MAR and OJI as the number of individual juniper trees per hectare (ind ha^{-1}) based on the three aerial photos. The first was an orthophoto in black and white that was taken in 1956 at a 1:33000 scale (Instituto Cartográfico de Andalucía, distributed by Red de Información Ambiental de Andalucía REDIAM; http://www.juntadeandalucia.es/medioambiente/site/rediam). The second was a digital panchromatic orthophoto that was dated 1977 at a 1:18 000 scale (Instituto Cartográfico de Andalucía) and the third was an orthophoto IRc that was dated 2005 at a 1:5000 scale (Remote sensing and GIS laboratory, Estación Biológica de Doñana, CSIC).

We estimated the density variations at each subplot (ΔD) from 1956 to 1977 by comparing the density values from the first and second images. Similarly, we obtained ΔD from 1977 to 2005 by comparing the second and third images. Hereafter, we will refer to the period (time-lag) spanning 1956–1977 as TL1 and to that from 1977 to 2005 as TL2. Because the study area became a protected national park in 1969, TL1 describes the population dynamics at an early colonization stage, and TL2 outlines the expansion patterns at an advanced colonization stage.

Different spatial scales and quality among the images led to spatial discrepancies. We georeferenced the 1956 and 1977 images using a set of landmarks (buildings, fences and roads) that were identifiable in a georeferenced 2005 photograph. This procedure reduced the spatial discrepancies from 6 to 7 m to < 2 m. To address the influence of image quality on density estimation, we first reduced the resolution of the IRc photograph (hereafter referred to as IRc-transformed) by increasing the pixel size from 0.5 to 1 m and generating a grey-scale image. Then, we identified juniper trees on an individual basis in the two images (IRc and IRc-transformed photos) and cross-checked these counts with previous data describing *in situ* mapped individuals to test the accuracy of our photointerpretation (Korpela 2004; Fretwell *et al.* 2012). The specific criteria for the identification of individual trees were based on shape, colour, definition and contrast as reported in Appendix S1 (Supporting Information). We then applied interpolation techniques to obtain two density maps that were based on the IRc and IRc-transformed photos and set 100 random points for each density map, from which the interpolated density values were recorded. Finally, we regressed the interpolated density values and the actual density value that was recorded *in situ*. Fitted models estimated the magnitudes of the potential biases that occurred due to the complexities of the vegetation structures, the expertise of the researcher in applying the photointerpretation methods, and the quality of the image (Korpela 2004). The estimated bias, which is usually an underestimation of the actual density, was subsequently applied to correct the estimated juniper density values that were based on the images from 1956, 1977 and 2005 (García *et al.* 2014). We used ARCGIS v. 9.3 (ESRI; Redlands, CA, USA) and the MASS library (Venables & Ripley 2002) that was implemented in R v. 2.13.0 (R Development Core Team 2010) to perform the photointerpretation of the aerial photos and to fit the regression models, respectively.

SPATIO-TEMPORAL DEMOGRAPHIC TRENDS AND THEIR ECOLOGICAL CORRELATES

Univariate and bivariate spatial indices of autocorrelations

We explored the spatio-temporal patterns of the covariation in density changes by testing for clustering at the plot level (based on Moran's *I*) and identifying local clusters within plots (based on local indicators of spatial aggregation). First, we tested for clustering (i.e. the presence of aggregates of similar or dissimilar ΔD values) at the plot level. We applied the Moran's *I* index, which is a global spatial autocorrelation function that measures the resemblance of pairs of values that are located within a set of predefined distances (Legendre & Legendre 2012). Our weighted matrix was set to $W_{hi} = 1$ when subplots were within 100 m distance of each other and $W_{hi} = 0$ otherwise. We chose 100 m as the connecting distance because this is the minimum distance that was necessary to avoid non-connected subplots given our sampling design. We also tested for increasing connecting distances and evaluated whether the Moran's tests yielded similar results. The expected value of Moran's *I* for no spatial correlation is $E(I) = -1/(n-1)$, in which n is the number of observations. When n is large, $E(I)$ tends to correspondingly decrease, with values above *E (I)* indicating positive correlations (i.e. spatial clustering of similar values) and values below *E (I)* denoting negative correlations (i.e. spatial clustering of dissimilar values). The statistical significance of the Moran's *I* index was estimated based on permutations ($N = 99\,999$, $P < 0.05$). We used the *spdep* package (Bivand 2013) that was implemented in R to estimate Moran's *I* and applied the Holm correction to the *P*-values for multiple testing to avoid increased type I errors.

The global Moran's *I* index offered a high-level summary of the spatial structures of ΔD values at the plot level but did not show the location of the aggregates with similar or dissimilar values within the study plots. To identify the local clusters of similar or dissimilar ΔD values compared with what would be expected by chance, we estimated the local indicators of spatial autocorrelation (LISA) value for each plot, which was based on the local Moran's index (Anselin 1995). We further visualized the results as a cluster map depicting the locations of the subplots that yielded local Moran's *I* values that were significantly higher or lower than zero based on 99999 permutations (pseudo-$P = 0.01$ after applying Bonferroni's correction to avoid increased type errors I according to Anselin (1995)). Thus, two main types of clusters were identified, including hotspots of regeneration that corresponded with clusters of subplots with high ΔD values and coldspots of regeneration that corresponded with clusters of subplots with low ΔD values. We also tested for the presence of two additional types of clusters showing significant dissimilar ΔD values between local and neighbouring subplots, such as the outliers of regeneration that were represented by subplots with high ΔD values that were surrounded by subplots with low ΔD values and gaps of regeneration that corresponded with subplots having low ΔD values that were surrounded by those with high ΔD values.

Multivariate spatial association tests assessed whether values for one variable (z_k) that were observed at a given location were spatially associated with another variable (z_l) that was observed at a neighbouring location (Borcard & Legendre 2012). We applied bivariate spatial autocorrelation analyses to test for the association between ΔD at a given subplot and the value of the initial density D_0 that was measured at a neighbouring subplot. These analyses thus tested for the spatial correlation between the mean ΔD value at a given subplot and the mean D_0 value at a neighbouring subplot. We used *GeoDa* (https://geodacenter.asu.edu) to estimate the local and global Moran's I indices of spatial autocorrelations to apply multivariate Moran's I and visualize cluster maps. Cluster maps were further represented using the visualization library *ggmap* (Kahle & Wickham 2013).

Ecological correlates driving density variations

For each subplot, we recorded the elevation (*Elev*), initial density that was registered in 1956 (D_0) and distance to the remnant forest (*Dist*). We chose these variables because they are known to influence population growth and they are measurable by GIS tools. To remove the spatial autocorrelations that typically lead to statistical biases (Keitt *et al.* 2002), we first detrended our response variable (ΔD) by fitting a generalized least square model (*gls*) with the spatial coordinates (X, Y) of the subplot as covariates. We further retained the standardized residuals that became our new response variable (ΔD_{res}) and fit a generalized additive mixed model (GAMM) with PLOT and TL as fixed-effect factors that were included in the full model together with D_0, *Elev* and *Dist* and their interaction terms as predictors. We also included the subplots as random factors and allowed for temporal-autocorrelated residuals because the data were recorded at two successive time-lags. We selected the best-fit model according to the AIC values to proceed with further model validations as described by Zuur *et al.* (2009). Residuals varied proportional to the power of the absolute value of the variance–covariance of D_0 to cope with any heteroscedasticity in relation to D_0 (Zuur *et al.* 2009). We fit the model according to REML, and our final model included only the significant factors and interaction terms influencing ΔD_{res}. We used the *mgcv* library (Wood 2006) that was implemented in R version 3.0.2 (R Development Core Team 2010) to fit the GAMM models and to select for the best-fit model and plot the estimated smoothing curves.

Results

VALIDATION OF PHOTOINTERPRETATION METHODS

Estimated density values that were based on high-resolution IRc images and low-resolution IRc-transformed images significantly correlated with the actual densities (i.e. *in situ* measurements), suggesting that the photointerpretation methods yielded reliable local density values ($P < 0.001$, Fig. S1 in Supporting Information). Note that β coefficients that are close to 1 indicate a strong resemblance between the estimated and actual density values. Most β coefficients were significantly lower than 1, indicating that the interpretation of aerial photos tended to underestimate the mean density values. More specifically, β coefficients tended to diminish from low- to medium- and high-density situations (β = 0.53 and $R^2_{adj} = 0.91$, β = 0.40 and $R^2_{adj} = 0.93$, and β = 0.32 and $R^2_{adj} = 0.95$), respectively, for the high-resolution images. At a given density level, low-resolution images consistently yielded less accurate density estimates compared with those that were obtained from high-resolution images. Low-resolution images yielded the least accurate density estimates, which particularly occurred in high-density situations (β = 0.23 and $R^2_{adj} = 0.91$).

UNIVARIATE AND BIVARIATE SPATIAL INDICES OF AUTOCORRELATIONS

Global Moran's indices were positive and significantly differed from zero within the first distance class; that is, subplots that were located < 100 m apart tended to have similar mean ΔD values, whereas the magnitude of the density change can be considered to be spatially independent among the subplots that were located over 100 m apart. The Moran's I index increased from TL1 to TL2 both for MAR (from 0.17 to 0.22) and OJI (from 0.28 to 0.36), involving an increased spatial clustering of ΔD values within each plot. Thus, subplots with significantly similar or dissimilar ΔD values tended to aggregate within each plot as colonization proceeded. Additional multivariate Moran's I values showed that a ΔD at a given subplot was significantly correlated with the neighbouring values of D_0 both for MAR and OJI for TL1 (Figs S2 and S3). Therefore, subplots with increased ΔD values were surrounded by those with large D_0 values for both MAR (Moran's $I = 0.35$, $P < 0.01$) and OJI (Moran's $I = 0.19$, $P < 0.05$) at the early colonization stage. The sign of this correlation changed during TL2 for MAR, indicating that subplots with strongly declining ΔD values tended to be surrounded by those with high D_0 values (Moran's $I = -0.26$, $P < 0.01$). This demographic trend was not observed for OJI because multivariate Moran's I values were not significantly different from zero during TL2 (Moran's $I = -0.12$, $P > 0.05$).

Overall, we identified six hotspots, two coldspots and two outliers of regeneration but failed to identify gaps of regeneration at $P < 0.01$ (Fig. 2). Specifically, we found hotspots at both plots and time-lags, but coldspots only arose during TL2 (1977–2005). Outliers of regeneration appeared both for MAR (during TL1) and OJI (during TL2). Therefore, we found similar numbers of hotspots, coldspots and outliers of regeneration for both plots, but the spatial locations of each type of cluster changed among the plots and time-lags (Fig. 2); for MAR, the hotspots of regeneration moved from northern locations (during TL1) to southern locations (during TL2). Interestingly, the subplot #M13 acted as a hotspot of regeneration during TL1 but became a coldspot during TL2 (Fig. 2).

ECOLOGICAL CORRELATES DRIVING DENSITY VARIATIONS

The best-fit model explained approximately 40% of the observed variance ($R^2_{adj} = 0.39$, Table 1). This model included TL as a main fixed factor, showing that ΔD_{res} increased during TL1 (β = 47.21, t-value = 2.02, $P < 0.05$), whereas ΔD_{res} showed an overall decrease at TL2 (β = −68.43, t-value = −2.42, $P < 0.05$). Regarding ecological correlates, the smoother for D_0 was significant at the 5% level, and

© 2014 The Authors. Journal of Ecology © 2014 British Ecological Society,

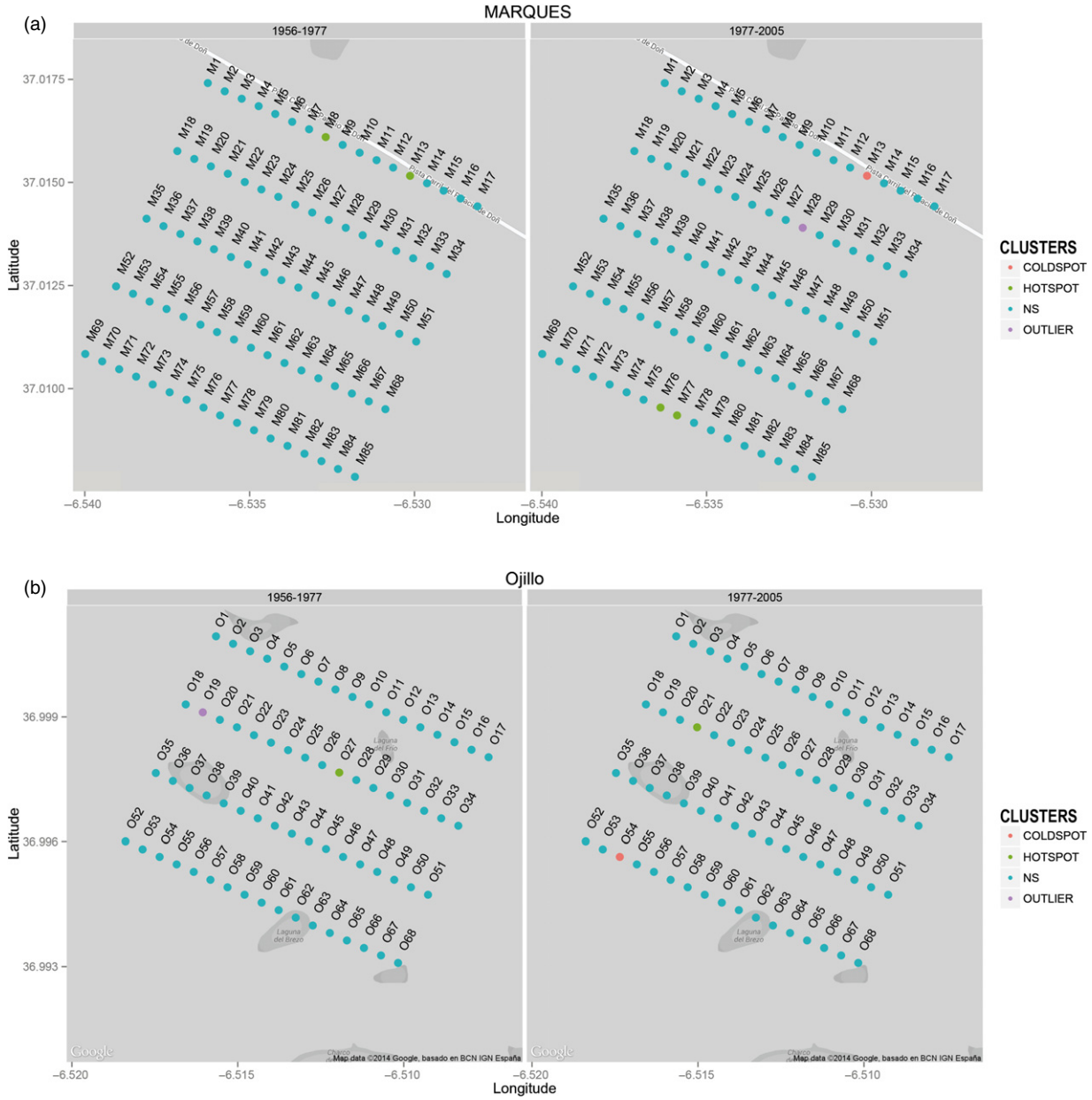

Fig. 2. Cluster maps by plot and time-lag. Each dot represents a subplot location, and the colours indicate the significance level of the associated local index of spatial autocorrelation (LISA) at MAR (a) and OJI (b) for both TL1 (1956–1977) and TL2 (1977–2005). Significant indices represent clusters of regeneration as follows: hotspots (green), coldspots (orange) and outliers (violet) of regeneration. Blue dots indicate a non-significant (NS) association between the local ΔD (measured at a given plot) and the average ΔD value measured at neighbouring plots based on permutation tests (N = 99 999, $P < 0.01$).

Fig. 3a shows that it had a positive effect on density variation in low-density situations (< 500 ind ha^{-1}) but caused population declines when initial densities exceeded 500 ind ha^{-1}. Our model also showed the contrasting effects of D_0 at different colonization stages. Although it had positive effects on ΔD_{res} across a wide range of density values during TL1 (Table 1, Fig. 3b), it failed to detect significant variation patterns of ΔD_{res} that were mediated by D_0 during TL2 (Table 1). *Dist* interacted with TL, and *Elev* interacted with PLOT to influence density variations. The effects of *Dist* as a proxy of distance limitation changed across the study chronosequence as expected; it slightly increased population growth when *Dist* = 0 (i.e. within remnant patches) during TL1, and it strongly correlated with population growth at *Dist* = −300 m for TL2, (Table 1, Fig. 3c). These results suggest that the population regenerated mainly within (or nearby) remnant forests at the early colonization stages, whereas it expanded preferentially westward with a strong density peak at 300 m from the mature forest at the late colonization stages. With regard to *Elev*, which was a proxy for soil moisture, our model indicates that the ΔD_{res} slightly increased at low elevations for MAR, as expected, but in contrast with our expectations, this parameter increased both at high and low elevations for OJI (Fig. 3d).

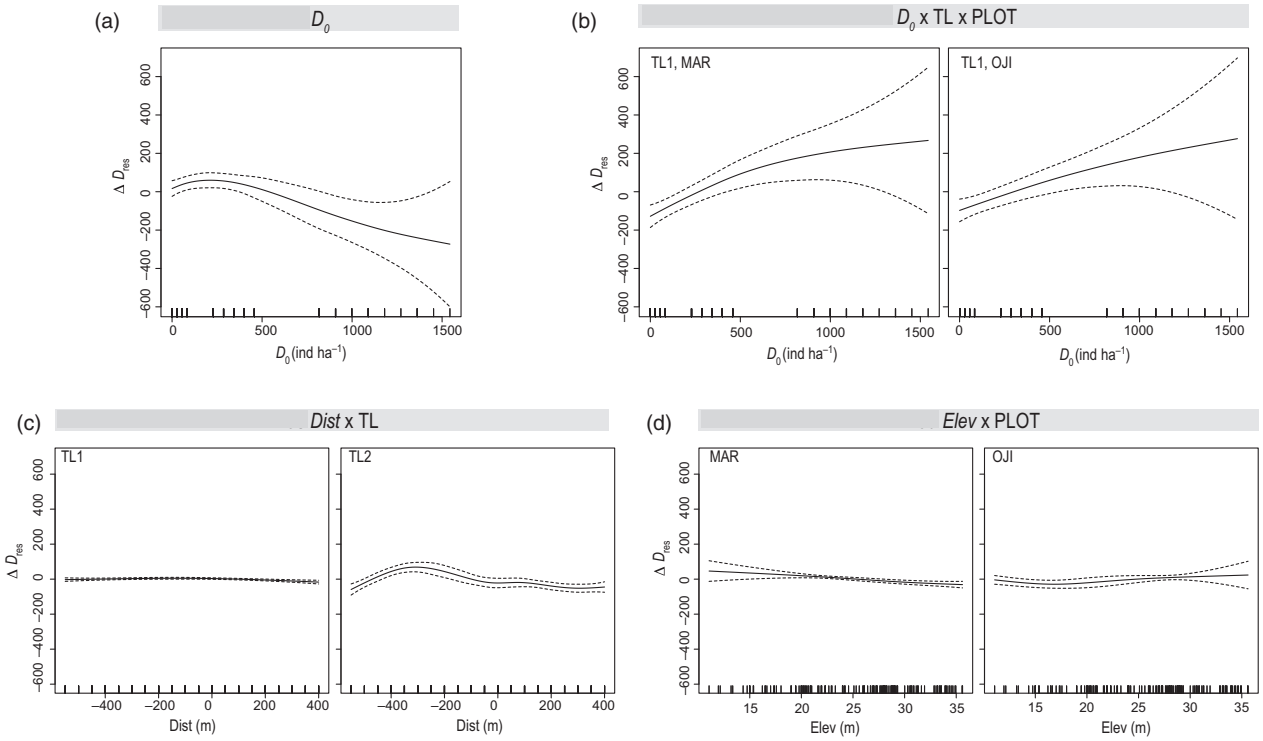

Fig. 3. Estimated smoothing curves for the best-fit model that contains D_0 as a smooth term and its interaction with TL and PLOT. The model also included the interaction terms *Dist* × TL and *Elev* × PLOT as explanatory variables. The *x*-axis shows the values of different ecological correlates (D_0, *Dist* and *Elev*), and the *y*-axis depicts the contribution of the smoother to the fitted values. The solid line represents the smoother, and the dotted lines depict 95% confidence bands. Marks on the *x*-axis are recorded values for each ecological correlate.

Discussion

The photointerpretation of the aerial images yielded reliable density data that, when combined with spatially explicit analyses, showed spatio-temporal demographic trends in the expanding populations. In spite of its workability, it is worth noting that photointerpretation poses some pitfalls. For example, we proved that low-resolution images yielded less accurate density estimates, and therefore, these data must be corrected by other means, including cross checking with *in situ* measurements. This requirement may represent a limitation for studies dealing with recently extirpated populations or those that are located in inaccessible areas (Fretwell *et al.* 2012). Our results indicated that the photointerpretation of aerial images tends to underestimate population densities and that this bias is especially severe in high-density situations. Therefore, the interpretation of aerial photos is most suitable for the addressing of demographic studies in open-canopy ecosystems, such as semi-arid Mediterranean forests, that allow for *in situ* measurements to correct biased estimates. Because these technical issues can be easily overcome, we envision that the photointerpretation of aerial images will be routinely incorporated into ecological forecasting protocols that track population responses to environmental and land-use changes (Clark *et al.* 2001).

Our results show an overall demographic expansion of the juniper woodland population over the course of five decades (1956–2005) in addition to a significant spatio-temporal variation in population trends. The juniper population greatly increased during the early colonization stage (TL1), but we observed increased intraplot spatial heterogeneity in population trends

Table 1. Parameter estimates of the best-fit model (generalized mixed additive regression model) with residual density variation (ΔD_{res}) as response variable, TL as a fix factor and D_0, *Elev* and *Dist* as smooth terms. We set the subplot as the random factor. The last column indicates the figure depicting the smoothing curves for each significant explanatory variable

	β-value	SE	*t*-value	*P*-value	Smoothing curve
Parametric estimates					
Intercept	47.21	23.34	2.023	< 0.05	
TL (1977–2005)	−68.43	28.23	−2.424	< 0.05	
	edf	***F***	***P*-value**		**Smoothing curve**
Approximate significance of smooth terms					
D_0	2.72	5.08	< 0.01		Fig. 3a
Dist: TL1	2.12	4.74	< 0.01		Fig. 3c
Dist: TL2	5.05	10.19	< 0.001		Fig. 3c
Elev: PLOT (MAR)	1.62	4.58	< 0.05		Fig. 3d
Elev: PLOT (OJI)	2.44	4.05	< 0.05		Fig. 3d
D_0: TL1: (MAR)	1.56	11.73	< 0.001		Fig. 3b
D_0: TL1: (OJI)	1.25	8.90	< 0.01		Fig. 3b
D_0: TL2: (MAR)	0	0.08	n.s.		
D_0: TL2: (OJI)	0	0.60	n.s.		

© 2014 The Authors. Journal of Ecology © 2014 British Ecological Society,

during the late colonization stage (TL2), which is when we recorded both the hotspots and coldspots of regeneration. Overall, we found evidence of nucleated patterns, which was expected for an endozoochorous species that is actively dispersed by medium-to large-sized vertebrates, which tend to create highly aggregated seed rain patterns. Our results indicate a significant influence of D_0, *Dist* and *Elev* on density variations across the landscape with differential effects of D_0 and *Dist* (as proxies of some type of dispersal limitation) at the early and the late colonization stages.

Spatial correlation analyses show that population expansion resulted in increased spatial clustering, which was supported by the elevated Moran's *I* values at TL2 compared with TL1, the disappearance of hotspots of regeneration at the core of the remnant forest and emergence of new hotspots at the colonization front, and the emergence of coldspots of regeneration at late colonization stages. These changes are most evident for MAR, where highly active subplots at TL1, including hotspots of regeneration (subplots #M1-#M17), were located at the northern transect, whereas the same subplots showed reduced or negative density variations during TL2 (Fig. 2a). Furthermore, subplot #M13 was a hotspot of regeneration during TL1 but became a coldspot of regeneration during TL2 (Fig. 3a). Therefore, this population tends to expand from the northern subplots (the core) to southern locations (the front wave) (Fig. S3 in Supporting Information). The demographic trends showed less contrast between the time periods at OJI, where the density steadily increased during TL2.

The expansion of juniper in the study area developed in a nucleated pattern as shown in Fig. 2, where outliers of regeneration emerged at the colonization front. Previous studies have reported nucleated colonization patterns in expanding populations of endozoochorous species as a result of the active movement of propagules from mature forests to peripheral areas (Verdú & García-Fayos 1996; Hampe *et al.* 2008; García & Martínez 2012). Nucleated patterns that are mediated by frugivores are prompted by some landscape features, including the following: (i) conspicuous trees where birds perch or rest (Schupp, Milleron & Russo 2002); (ii) soft, linear structures, such as roads or trails that are recurrently used by mammals (Suarez-Esteban, Delibes & Fedriani 2013; Suárez-Esteban, Delibes & Fedriani 2013); and (iii) clumps of diverse arrays of fleshy fruit tree species on which frugivorous vertebrates frequently feed (Clark *et al.* 2004; Carlo & Morales 2008). An ongoing study in the same area demonstrated that stone pine trees are more abundant at OJI than at MAR and that these trees are frequently used for perching by frugivorous birds, which may explain the relatively steady density variation at OJI. Overall, these results show that the colonization patterns fit the nucleated patterns that are expected for expanding populations of endozoochorous species. In agreement with recent studies, our findings demonstrate that plant-animal mutualisms buffer the detrimental outcomes of anthropogenic fragmentation by providing dispersal services and enhancing quick forest recovery after light or moderate anthropogenic disturbances (Jordano *et al.* 2007; Montoya *et al.* 2008; Zamora *et al.* 2010; Bustamante-Sánchez & Armesto 2012; García & Martínez 2012; Markl *et al.* 2012).

Our study identified key ecological correlates in addition to dispersal by frugivores that underlie expansion patterns. These factors did not influence density variation uniformly throughout the study chronosequence as we had hypothesized. Thus, factors ameliorating propagule or distance limitations, such as elevated D_0 (initial density) or shorter *Dist* (distance to the remnant patch) values, should have a strong influence during the early colonization stage (TL1) (Harper 1977; Crawley 2007). Accordingly, higher D_0 values were associated with enhanced population growth during TL1, but we failed to detect any significant trends during TL2. However, the overall effects of D_0 demonstrate that increased initial densities resulted in population declines, which in some cases even reached negative values in high-density situations (Fig 3a). It is likely that the high intraplot heterogeneity in density variation that was observed at TL2 limited our ability to identify significant demographic trends that were mediated by D_0 during the late colonization stages. Furthermore, the bivariate spatial indices of autocorrelation indicate that the D_0 values that were measured at neighbouring subplots also influenced the density variation at a given subplot (Fig. S2). Therefore, the amplitude of density variation in a given subplot is not merely explained by the combination of factors that exist in a given subplot. It is necessary to account for the additional influences of the surrounding to understand the responses of populations to land-use changes. The other variable implying dispersal limitation, *Dist*, also showed differential effects in the early and late colonization stages. The population grew modestly near the remnant forest (*Dist* ~ 0 m) and increased farther from the mature forest (at a preferentially westbound distance of approximately 300 m) during TL2. Svenning *et al.* (2014) suggested that plant abundances are not continuous or homogeneous at the margins of their geographic ranges (leading fronts or rear edges) as these margins represent newly colonized landscapes. This observation has profound implications in predicting the distribution of expanding species in response to forthcoming climate-driven changes.

Our results suggest that *Elev* (a proxy of soil moisture) also influences population growth and has differential effects between plots but not between time periods (TL). We expected that subplots at low elevations would show increased population growth compared with those that were located at high elevations because they were closer to the underground water-table. This expected trend was observed at MAR but was not obvious at OJI, where population growth slightly increased at low and high elevations and subtly decreased at mid-level elevations. This contrasting effect of *Elev* on population trends between plots, rather than time-lags, may be explained by the drier conditions at MAR compared to OJI. A survey of the resident species at each plot showed that dominant woody species, such as *H. commutatum* and *H. halimifolium*, tended to inhabit more xeric sites in the study area, whereas the shrub species inhabiting OJI, such

as *E. scoparia* and *U. minor*, prefer more mesic conditions (C. García, pers. obs.).

Thus, long-term pattern-driven studies have revealed the ecological correlates that underlie demographic trends and to what extent their effects change across the landscape and/or throughout the study chronosequence. We have documented the long-term colonization patterns of populations inhabiting managed landscapes and discussed the role of spatio-temporal factors in driving colonization patterns that are associated with land-use changes. The interpretation of aerial photos in combination with spatial statistics allow for ecological researchers to investigate the population dynamics of key species; that is, foundation species in semi-arid conditions. Furthermore, this strategy can be applied to decipher the relative influences of climate changes versus land-use changes in driving vegetation dynamics. This is an important issue in forest ecology because recent studies have revealed pole-ward shifts in the distributions of forest species in response to climate change. However, these demographic expansions may be related to land-use changes that favour the colonization of deforested areas and abandoned rural lands (Bodin *et al.* 2013). Moreover, the ability to identify hotspots, outliers and coldspots of regeneration provides highly valuable information for the prediction of species-specific demographic trends in response to extreme drought, such as that which has been reported for juniper woodlands (Lloret & Granzow 2013), in addition to their potential effects on the ecosystem. Finally, by identifying the colonization front at different time-lags and using genomic tools, we could investigate climate-induced population-adaptive responses at the colonization wave front (van Mantgem & Stephenson 2007; Excoffier, Foll & Petit 2008). A wide range of genomic tools are currently available in forestry research for model species (Neale & Kremer 2011) that may be used to address important ecological questions, particularly for foundation species.

Acknowledgements

We are indebted to E. W. Schupp, two anonymous referees, and the Handling Editor of this manuscript for their valuable suggestions in reviewing this paper. This work was funded by Fundação para a Ciência e a Tecnologia (FCT) (PTDC/BIA-ECS/116521/2010) and cofunded by the European Program COMPETE: FCOMP-01-0124-FEDER-019772, which was granted to CG. It was also supported by the project '*Genomics and Evolutionary Biology*', which was cofinanced by the North Portugal Regional Operational Programme 2007/2013 (ON.2 – O Novo Norte) under the National Strategic Reference Framework (NSRF), through the European Regional Development Fund (ERDF). EM was supported by the Ministerio de Ciencia y Tecnología (MICINN) with a doctoral grant (BES-2011 044380). PJ was supported by a Junta de Andalucía Excellence Grant (RNM-5731) in addition to a Severo Ochoa Excellence Award from the Ministerio de Economía y Competitividad (SEV-2012-0262). We particularly acknowledge the Doñana Monitoring Team of Estación Biológica de Doñana and the LAST facilities, who made the long-term ecological research in the Doñana LTSER Platform possible, and the Ministry of Environment and Junta de Andalucía, who also provided funding. Aerial photos were provided by the Instituto Cartográfico de Andalucía and REDIAM.

Data accessibility

Data deposited in the Dryad repository: http://datadryad.org/resource/doi:10.5061/dryad.m184s (García *et al.* 2014).

References

Adams, R.P. (2011) *Junipers of the World: The Genus Juniperus*. Trafford, Bloomington.

Allier, C., González, F. & Ramirez, L. (1974) *Mapa ecológico de la Reserva Biológica de Doñana*. CSIC, Sevilla.

Anselin, L. (1995) Local indicators of spatial association-LISA. *Geographical Analysis*, **27**, 93–115.

Bivand, R. (2013) spdep: Spatial dependence: weighting schemes, statistics and models. R package version 0.5-68.

Bodin, J., Badeau, V., Bruno, E., Cluzeau, C., Moisselin, J.-M., Walther, G.-R. & Dupouey, J.-L. (2013) Shifts of forest species along an elevational gradient in Southeast France: climate change or stand maturation? *Journal of Vegetation Science*, **24**, 283.

Borcard, D. & Legendre, P. (2012) Is the Mantel correlogram powerful enough to be useful in ecological analysis? A simulation study. *Ecology*, **93**, 1473–1481.

Bustamante-Sánchez, M.A. & Armesto, J.J. (2012) Seed limitation during early forest succession in a rural landscape on Chloé Island, Chile: implications for temperate forest restoration. *Journal of Applied Ecology*, **49**, 1103–1112.

Carlo, T.A. & Morales, J.M. (2008) Inequalities in fruit-removal and seed dispersal: consequences of bird behaviour, neighbourhood density and landscape aggregation. *Journal of Ecology*, **96**, 609–618.

Clark, J.S., Carpenter, C., Barber, M., Collins, S., Dobson, A., Foley, J.A. *et al.* (2001) Ecological forecasting: an emerging imperative. *Science*, **293**, 657–660.

Clark, C.J., Poulsen, J.R., Connor, E.F. & Parker, V.T. (2004) Fruiting trees as dispersal foci in a semi-deciduous tropical forest. *Oecologia*, **139**, 66–75.

Condit, R., Ashton, P.S., Manokaran, N., LaFrankie, J.V., Hubbell, S.P. & Foster, R.B. (1999) Dynamics of the forest communities at Pasoh and Barro Colorado: comparing two 50-ha plots. *Philosophical Transactions of the Royal Society of London Series B-Biological Sciences*, **354**, 1739–1748.

Crawley, M.J. (2007) *Plant Population Dynamics*. Oxford University Press, Oxford, UK.

Dellafiore, C.M., Valles, S.M. & Fernandez, J.B.G. (2006) Rabbits (*Oryctolagus cuniculus*) as dispersers of *Retama monosperma* seeds in a coastal dune system. *Ecoscience*, **13**, 5–10.

Díaz-Delgado, R. (2010) An integrated monitoring programme for Doñana Natural Space: The set-up and implementation. *Conservation Monitoring in Freshwater Habitats: A Practical Guide and Case Studies* (eds C. Hurford, M. Schneider & I. Cowx), pp. 339–355. Springer Science and Business Media, Dordrecht.

Excoffier, L., Foll, M. & Petit, R.J. (2008) Genetic consequences of range expansions. *Annual Review of Ecology, Evolution, and Systematics*, **40**, 481–501.

Fedriani, J.M. & Delibes, M. (2009) Functional diversity in fruit-frugivore interactions: a field experiment with Mediterranean mammals. *Ecography*, **32**, 983–992.

Foster, D.R. (2002) Insights from historical geography to ecology and conservation: lessons from the New England landscape. *Journal of Biogeography*, **29**, 1269–1275.

Fretwell, P.T., LaRue, M.A., Morin, P., Kooyman, G.L., Wienecke, B., Ratcliffe, N., Fox, A.J., Fleming, A.H., Porter, C. & Thrathan, P.N. (2012) An emperor penguin population estimate: the first global, synoptic survey of a species from space. *PLoS ONE*, **7**, 1–11.

García, D. & Martínez, D. (2012) Species richness matters for the quality of ecosystem services: a test using seed dispersal by frugivorous birds. *Proceedings of the Royal Society B: Biological Sciences*, **279**, 3106–3113.

García, C., Moracho, E., Díaz-Delgado, R. & Jordano, P. (2014) Data from: Long-term expansion of juniper populations in managed landscapes: patterns in space and time. *Dryad Digital Repository*, doi:10.5061/dryad.m184s.

García-Novo, F. & Merino, J. (1997) Pattern and process in the dune system of the Doñana National Park, Southwestern Spain. *Ecosystems of the World* (ed. E. van der Maarel), pp. 97–116. Elservier, Amsterdam.

Getzin, S., Wiegand, T., Wiegand, K. & He, F. (2008) Heterogeneity influences spatial patterns and demographics in forest stands. *Journal of Ecology*, **96**, 807–820.

González-Bernáldez, F., García-Novo, F. & Ramírez, L. (1975a) Analyse factorielle de la végétation de dunes de la Reserve Biologique de Doñana (Espagne). I. Analyse numerique des donnes floristiques. *Israel Journal of Botany*, **24**, 106–117.

González-Bernáldez, F., García-Novo, F. & Ramírez, L. (1975b) Analyse factorielle de la végétation de dunes de la Reserve Biologique de Doñana (Espagne). II. Analyse numerique des donnes floristiques. *Israel Journal of Botany*, **24**, 173–182.

© 2014 The Authors. Journal of Ecology © 2014 British Ecological Society,

Granados, M.A., Martín, A. & García-Novo, F. (1988) Long term vegetation changes on the stabilized dunes of Doñana National Park (SW Spain). *Vegetatio*, **75**, 73–80.

Hampe, A., García-Castaño, J.L., Schupp, E.W. & Jordano, P. (2008) Spatio-temporal dynamics and local hotspots of initial recruitment in vertebrate-dispersed trees. *Journal of Ecology*, **96**, 668–678.

Harper, J.L. (1977) *Population Biology of Plants*. Academic Press, London.

Jordano, P. (1991) Gender variation and expression of monoecy in *Juniperus phoenicea* (L) (Cupressaceae). *Botanical Gazette*, **152**, 476–485.

Jordano, P. (1993) Geographical ecology and variation of plant-seed disperser interactions - Southern Spanish junipers and frugivorous thrushes. *Vegetatio*, **108**, 85–104.

Jordano, P., García, C., Godoy, J.A. & García-Castaño, J.L. (2007) Differential contribution of frugivores to complex seed dispersal patterns. *Proceedings of the National Academy of Sciences of the USA*, **104**, 3278–3282.

Kahle, D. & Wickham, H. (2013) ggmap: A package for spatial visualization with Google Maps and OpenStreetMap. R package version 2.3.

Kareiva, P.M., Kingsolver, J.G. & Huey, R.B. (1993) *Biotic Interactions and Global Change*. Sinauer Associates Inc., Massachusetts, MA.

Keitt, T.H., Bjornstad, O.N., Dixon, P.M. & Citron-Pousty, S. (2002) Accounting for spatial pattern when modeling organism-environment interactions. *Ecography*, **25**, 616–625.

Korpela, I. (2004) Individual tree measurements by means of digital aerial photogrammetry. *Silva Fennica*, **3**, 1–93.

Ladwig, L.M. & Meiners, S.J. (2010) Spatiotemporal dynamics of lianas during 50 years of succession to temperate forest. *Ecology*, **91**, 671–680.

Leadley, P., Pereira, H.M., Alkemade, R., Fernandez-Manjarrés, J.F., Proença, V., Scharlemann, J.P.W. & Walpole, M.J. (2010) Biodiversity Scenarios: Projections of 21st century change in biodiversity and associated ecosystem services. Technical Series, pp. 132. Secretariat of the Convention on Biological Diversity, Montreal.

Legendre, P. & Legendre, L. (2012) *Numerical Ecology*. Elsevier, Oxford.

Lloret, F. & Granzow, I. (2013) Plant competition and facilitation after extreme drought episodes in Mediterranean shrubland: does damage to vegetation cover trigger replacement by juniper woodland? *Journal of Vegetation Science*, **24**, 1020–1032.

van Mantgem, P.J. & Stephenson, N.L. (2007) Apparent climatically induced increase of tree mortality rates in a temperate forest. *Ecology Letters*, **10**, 909–916.

Markl, J.S., Schleuning, M., Forget, P.M., Jordano, P., Lambert, J.E., Traveset, A., Wright, J. & Böhning-Gaese, K. (2012) Meta-Analysis of the effects of human disturbance on seed dispersal by animals. *Conservation Biology*, **26**, 1072–1081.

Montoya, D., Zavala, M.A., Rodríguez, M.A. & Purves, D.W. (2008) Animal *versus* wind dispersal and the robustness of tree species to deforestation. *Science*, **320**, 1502–1504.

Muñoz-Reinoso, J.C. (2001) Vegetation changes and groundwater abstraction in SW Doñana, Spain. *Journal of Hydrology*, **242**, 197–209.

Neale, D.B. & Kremer, A. (2011) Forest tree genomics: growing resources and applications. *Nature Reviews*, **12**, 111–122.

Rau, J.R. (1987) *Ecología del zorro (Vulpes vulpes) en la Reserva Biológica de Doñana, Huelva*. PhD Universidad de Sevilla, SO de España.

R Development Core Team (2010) *R: A Language and Environment for Statistical Computing*. R Foundation for Statistical Computing, Vienna, Austria.

Rivas-Martínez, S., Costa, M., Castroviejo, S. & Valdés, E. (1980) La vegetación de Doñana (Huelva, España). *Lazaroa*, **2**, 5–190.

Schupp, E.W. (1995) Seed seedling conflicts, habitat choice, and patterns of plant recruitment. *American Journal of Botany*, **82**, 399–409.

Schupp, E.W., Milleron, T. & Russo, S.E. (2002) Dissemination limitation and the origin and maintenance of species rich tropical forest. *Seed Dispersal and Frugivory* (eds D.J. Levey, W.R. Silva & M. Galletti), pp. 19–33. CABI Publishing, Wallingford.

Seidler, T.G. & Plotkin, J.B. (2006) Seed dispersal and spatial pattern in tropical trees. *PLoS Biology*, **4**, 2132–2137.

Suarez-Esteban, A., Delibes, M. & Fedriani, J.M. (2013) Unpaved road verges as hotspots of fleshy-fruited shrub recruitment and establishment. *Biological Conservation*, **167**, 50–56.

Suárez-Esteban, A., Delibes, M. & Fedriani, J.M. (2013) Barriers or corridors? The overlooked role of unpaved roads in endozoochorous seed dispersal. *Journal of Applied Ecology*, **50**, 767–774.

Svenning, J.-C., Gravel, D., Holt, R.D., Schurr, F.M., Thuiller, W., Münkemüller, T. *et al.* (2014) The influence of interspecific interactions on species range expansion rates. *Ecography*, **37**, 1–12.

Valverde, J.A. (1958) An ecological sketch of the Coto Doñana. *British Birds*, **51**, 1–23.

Venables, W.N. & Ripley, B.D. (2002) *Modern Applied Statistics with S*. Springer, New York.

Verdú, M. & García-Fayos, P. (1996) Nucleation processes in a Mediterranean bird-dispersed plant. *Functional Ecology*, **10**, 275–280.

Watt, A.S. (1947) Pattern and Process in the plant community. *Journal of Ecology*, **35**, 1–22.

Whitham, T.G., Bailey, J.K., Schweitzer, J.A., Shuster, S.M., Bangert, R.K., Leroy, C.J. *et al.* (2006) A framework for community and ecosystem genetics: from genes to ecosystems. *Nature Reviews Genetics*, **7**, 510–523.

Williams, A.P., Allen, C.D., Millar, C.I., Swetnam, T.W., Michaelsen, J., Still, C.J. & Leavitt, S.W. (2010) Forest responses to increasing aridity and warmth in the southwestern United States. *Proceedings of the National Academy of Sciences*, **107**, 21289–21294.

Wood, S.N. (2006) *Generalized Additive Models: An Introduction with R*. Chapman and Hall, Boca Raton, Florida.

Yarranton, G.A. & Morrison, R.G. (1974) Spatial dynamics of primary succession: nucleation. *Journal of Ecology*, **62**, 417–428.

Zamora, R., Hódar, J.A., Matías, L. & Mendoza, I. (2010) Positive adjacency effects mediated by seed disperser birds in pine plantations. *Ecological Applications*, **20**, 1053–1060.

Zuur, A., Ieno, E.N., Walker, N., Savaliev, A.A. & Smith, G.M. (2009) Mixed effects models and extensions in ecology with R. Springer, New York.

Received 16 June 2014; accepted 14 July 2014
Handling Editor: Glenn Matlack

Supporting Information

Additional Supporting Information may be found in the online version of this article:

Appendix S1. Criteria for the identification and digitalization of individual trees.

Figure S1. Regression curves between the density estimates *in situ* (actual density) and those that were estimated from the IRc and IRc-transformed images.

Figure S2. Relationships between the normalized ΔD values at each subplot and the normalized D_0 values at the neighbouring subplots.

Figure S3. Density variation map at MAR (A) and OJI (B) for TL1 (1956–1977) and TL2 (1977–2005).

Supplementary on line material (SOM)

Annex 1. Criteria for identification and digitalization of individual trees were based on the shape, colour, definition and contrast.

We applied the following criteria for each ortophoto:

- Orthophoto 1956 B/W: Visualization scale on screen 1:1070. We identified as adult juniper trees circular spots more than 4 pixels size and digital pixel intensity values < 40. This image was analysed with the software ImageJ, that identifies pixels under a given threshold value, as recommended for B/W and low contrast images.

- Orthophoto 1977 B/W: Visualization scale on screen 1:670. We identified as adult individuals circular spots larger than 4 pixels size and digital values of <40 (*MAR* plot) and <70 (*OJI* plot).

- Orthophoto 2005 IRc: visualization scale on screen 1:270 where: *(i)* Large-sized individuals are characterized by a well-defined circular shaped spot coloured in dull red with a shadow projected to the NW; and *(ii)* Small-sized individuals are characterized by a circular-shaped spot coloured in dull red that contrasts with the grey colour of the open ground. We did not consider spots smaller than 9 pixels.

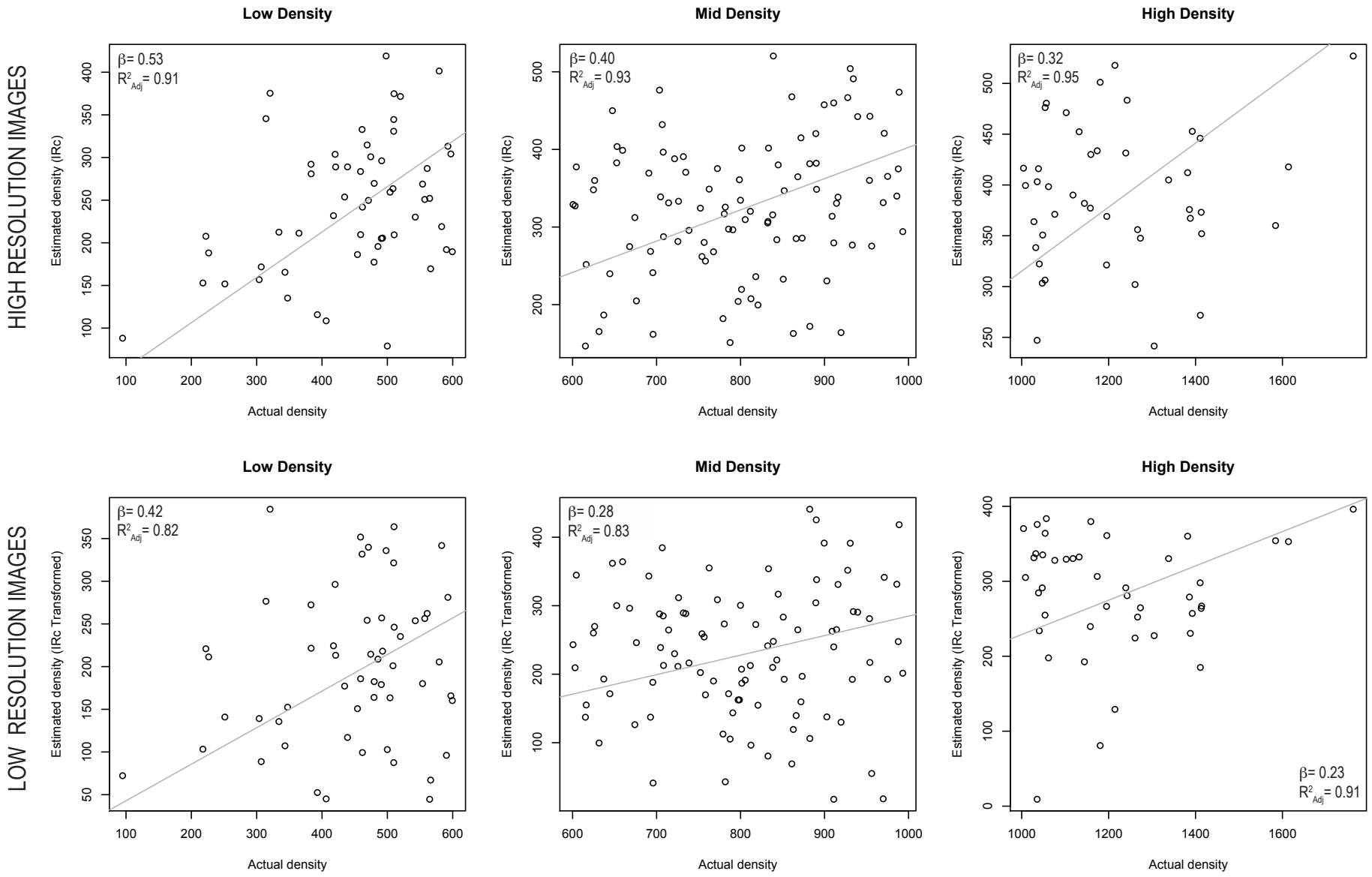

Fig. 1. SOM García et al. 2014

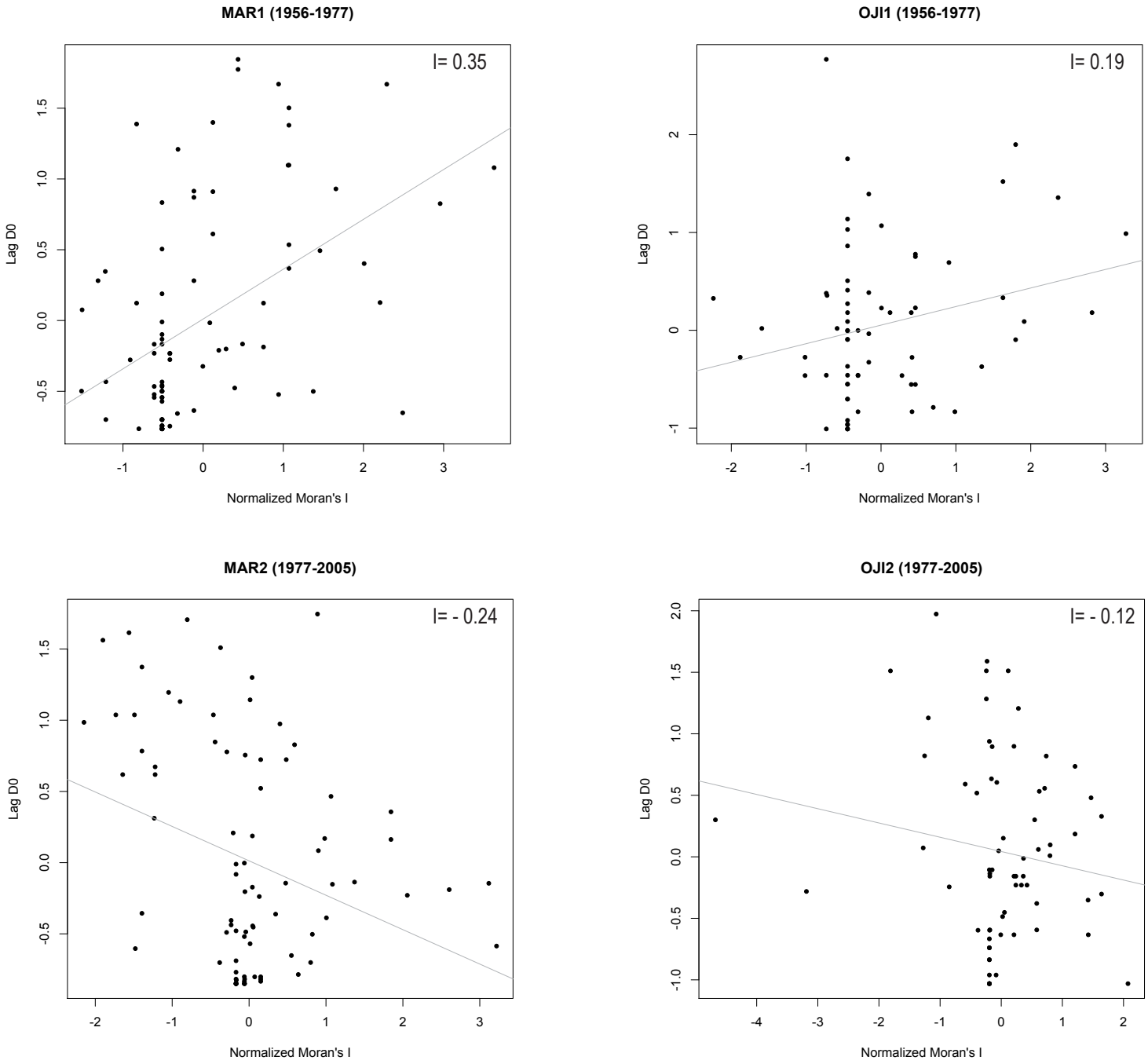

Fig 2 SOM García *et al.* 2014

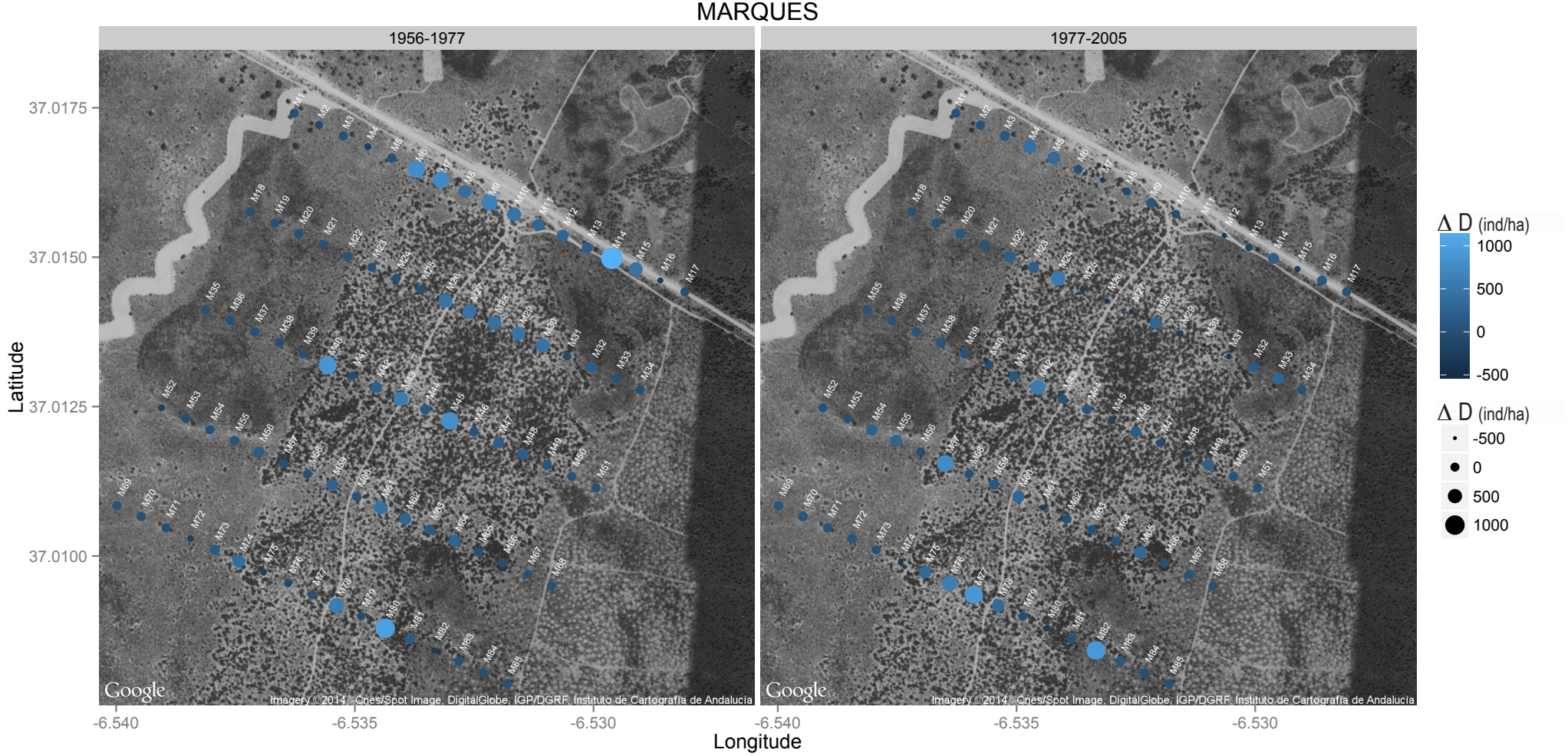
MARQUES
1956-1977
1977-2005
Latitude
Longitude
37.0175
37.0150
37.0125
37.0100
-6.540
-6.535
-6.530
Google
Imagery ©2014 , Cnes/Spot Image, DigitalGlobe, IGP/DGRF, Instituto de Cartografía de Andalucía
Δ D (ind/ha)
1000
500
0
-500
Δ D (ind/ha)
-500
0
500
1000

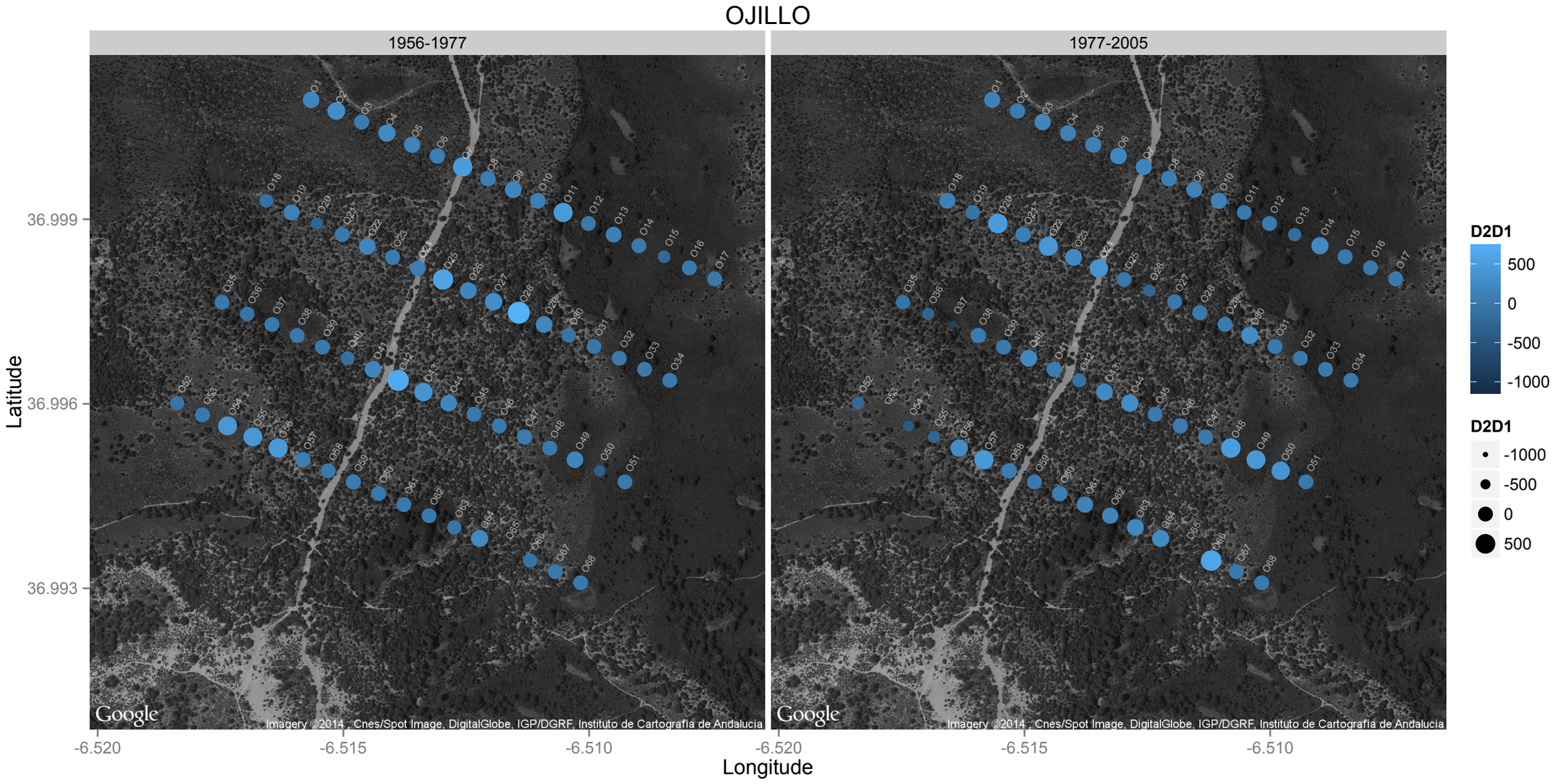
OJILLO
1956-1977
1977-2005
Latitude
36.999
36.996
36.993
-6.520
-6.515
-6.510
Longitude
Google
Imagery ©2014 , Cnes/Spot Image, DigitalGlobe, IGP/DGRF, Instituto de Cartografía de Andalucía
D2D1
500
0
-500
-1000
D2D1
-1000
-500
0
500